ACADEMIC PRESS

Available online at www.sciencedirect.com
SCIENCE DIRECT®

Journal of Catalysis 218 (2003) 148–154

JOURNAL OF CATALYSIS

www.elsevier.com/locate/jcat

Low-temperature deep oxidation of dichloromethane and trichloroethylene by H-ZSM-5-supported manganese oxide catalysts

J.I. Gutiérrez-Ortiz, R. López-Fonseca, U. Aurrekoetxea, and J.R. González-Velasco *

Departamento de Ingeniería Química, Facultad de Ciencias, Universidad del País Vasco/EHU, PO Box 644, E-48080 Bilbao, Spain

Received 31 October 2002; revised 13 February 2003; accepted 13 February 2003

Abstract

The catalytic activity and selectivity of a series of H-ZSM-5-supported manganese oxide catalysts with various manganese content, namely 1.0, 4.3, and 8.3 wt%, were evaluated for the oxidation of dichloromethane (DCM) and trichloroethylene (TCE). Previously, the highly active performance of H-ZSM-5 zeolite with respect to other supports, such as alumina and silica, was demonstrated, pointing out that the acidic properties of the support along with a high metallic dispersion of the resultant catalyst were key factors conditioning the catalytic performance. Mn(4.3%)/H-ZSM-5 catalyst was found to be an optimum catalyst for the combustion of both single and double carbon chlorinated compounds achieving $> 95\%$ conversion levels at temperatures between 400 and 450 °C. The major oxidation products were carbon monoxide, carbon dioxide, hydrogen chloride, and chlorine. It was observed that high manganese loadings led to increasing amounts of carbon dioxide and chlorine.

Keywords: Catalytic oxidation; Dichloromethane; Trichloroethylene; Manganese-supported catalysts; H-ZSM-5 zeolite; Alumina; Silica

1. Introduction

Chlorinated volatile organic compounds (VOCs), such as dichloromethane (DCM) and trichloroethylene (TCE), constitute a significant fraction of the hazardous air and water pollutants due to their inertness and their widespread application in industry [1]. Among the various disposal methods applicable for these chlorocarbons, low-temperature catalytic oxidation has recently gained interest [2]. The desired reaction is the complete reaction of the chlorinated VOC to produce HCl and CO_2. The catalyst used must be active in the destruction of a wide range of chlorinated compounds, including toxic by-products that can result from incomplete combustion.

Traditionally, supported transition metal oxides have been proposed as potential substitutes for noble metal-based catalysts [3]. Metal oxides are in general less active than noble metals but they resist deactivation by poisoning to a larger extent [4]. Among these systems chromium-based catalysts have exhibited the highest activity for chlorinated VOC abatement [5,6]. Nevertheless, the use of this type of catalysts tends to be restricted owing to the formation at low temperatures of extremely toxic residues such as chromium oxychloride [7]. Interestingly, supported manganese oxides have been proposed as cheap, environmentally friendly and efficient catalysts for catalytic decomposition of nonchlorinated VOCs [8,9]. However, less consideration has been given to investigating the suitability of such catalysts for chlorinated VOC destruction [10,11].

On the other hand, it is reported in the literature that both noble metal and metal oxides have been extensively used for the combustion of chlorinated hydrocarbons using alumina and silica as supports. Nevertheless, there are only few investigations about this type of reactions over metal-modified ZSM-5 zeolites [12,13]. As compared to alumina and silica, ZSM-5 zeolites have a high internal surface area (300–550 $m^2\,g^{-1}$), and a modest concentration of Brønsted sites, which are primarily of high strength. In addition, since ZSM-5 zeolites have fixed dimensions, the metal particle size distribution can be controlled in an appropriate way.

Hence, the present study focuses on the activity and product selectivity of H-ZSM-5-supported manganese oxide catalysts in the vapor-phase oxidation of dichloromethane and trichloroethylene under excess of dry air between 200 and 550 °C.

* Corresponding author.
E-mail address: iqpgovej@lg.ehu.es (J.R. González-Velasco).

0021-9517/03/$ – see front matter
doi:10.1016/S0021-9517(03)00142-8

2. Materials and methods

2.1. Catalyst preparation

The zeolite NH_4-ZSM-5 CBV5524G was supplied by the Zeolyst Corporation. The H-ZSM-5 zeolite (Si/Al = 27.3) was obtained by calcining the NH_4-ZSM-5 zeolite in air at 550 °C for 3 h. Manganese oxide-based zeolite catalysts were prepared by impregnation with manganese (II) nitrate tetrahydrate (Merck). In order to obtain the desired manganese loadings (1.0, 4.3, and 8.3 wt%, respectively), the concentration of precursor aqueous solutions were adjusted accordingly. The zeolite to impregnation solution ratio employed was 1:20.

After drying for 5 h at 120 °C in a convective oven, all the catalysts were activated by calcination at 550 °C in a furnace with air for 3 h. As a result, fairly homogenously colored batches from pale tan to dark brown were obtained. Then, the powdered catalysts were pelletized using a hydraulic press (Specac), and afterward these pellets were crushed and sieved to grains that were 0.3–0.5 mm in diameter.

2.2. Catalyst characterization

The manganese content in the catalysts was measured by inductively coupled plasma (ICP) spectroscopy in an ARL Fisons 3410+ICP equipment. Thermogravimetric (TG) analysis was carried out using an automatically recording Perkin Elmer TGS-2 thermobalance, using a linear heating rate of 10 °C min^{-1} in a dynamic atmosphere of air (50 ml min^{-1}).

The surface area and pore volume of the catalysts were determined by N_2 adsorption–desorption at −196 °C in a Micromeritics ASAP 2010 equipment. Samples were previously evacuated overnight at 450 °C under high vacuum. The adsorption data were treated with the full BET equation. Oxygen chemisorption measurements were performed at 300 °C using the same volumetric apparatus. The irreversible uptake of O_2 was measured using a dual isotherm, the samples were evacuated at 300 °C, and a second isotherm was obtained. The difference between the two isotherms accounts for the amount of oxygen irreversibly held on the catalyst surface.

X-ray diffraction (XRD) studies were carried out on a Philips PW 1710 X-ray diffractometer with Cu-K_α radiation ($\lambda = 1.5406$ Å) and Ni filter. The X-ray tube was operated at 30 kV and 20 mA. Samples were scanned from 2θ equal to 2° up to 60° and the X-ray diffraction line positions were determined with a step size of 0.02° and a counting time of 2.5 s per step.

Temperature-programmed desorption (TPD) of ammonia was performed on a Micromeritics AutoChem 2910 instrument. Prior to adsorption experiments, the samples were first pretreated in a quartz U-tube in a nitrogen stream at 550 °C for 30 min, and then they were cooled down to 100 °C. After admitting small pulses of ammonia in He at 100 °C up to saturation, the desorption was carried out from 100 to 550 °C at a heating rate of 10 °C min^{-1} in an He stream (50 cm^3 min^{-1}). This temperature was maintained for 15 min until the adsorbate was completely desorbed. The experimental procedure is described elsewhere [14].

Temperature-programmed reduction experiments were also carried out using a Micromeritics AutoChem 2910 instrument. Prior to reduction, the samples were first oxidized in a stream of 5% O_2/He (50 cm^3 min^{-1}) at 550 °C for 30 min. Afterward, they were cooled down to 50 °C in flowing nitrogen. The reduction was conducted from 50 to 1050 °C at a linear ramp of 10 °C min^{-1} in a 5% H_2/Ar stream. The apparatus was equipped with a drier to remove water from the reduction process and a TCD detector to measure the H_2 consumption.

2.3. Catalytic activity measurement

Oxidation reactions were carried out in a conventional fixed-bed reactor under atmospheric pressure. The flow rate through the reactor was set at 500 cm^3 min^{-1} and the gas hourly space velocity (GHSV) was maintained at 15,000 h^{-1}. The feed stream to the reactor was prepared by delivering the liquid chlorinated hydrocarbon (1000 ppm) by a syringe pump into dry air, which was metered by a mass flow controller. Details about the experimental procedure for reaction product analysis are described elsewhere [15].

3. Results and discussion

3.1. Catalyst characterization

TG analysis of manganese (II) nitrate tetrahydrate was performed in order to determine the effect of calcination temperature on the final state of the manganese oxide. In addition, XRD measurements of the precursor salt calcined at different temperatures (400, 550, and 700 °C) for 3 h in air were recorded. The identification of the oxide phases was carried out by a comparison to the JCPDS (Joint Committee on Powder Diffraction Standards) files.

TG results indicated that heating the precursor salt in air from 50 to 250 °C resulted in a significant weight loss (about 65%) which was associated with the $Mn(NO_3)_2 \cdot 4H_2O$–MnO_2 transformation. Indeed, the XRD results revealed the formation of MnO_2 as a major phase when calcining the precursor salt at 400 °C (Fig. 1). Increasing the temperature completely converted MnO_2 into Mn_2O_3 at around 550–600 °C. Accordingly, XRD analysis showed that Mn_2O_3 became the sole detectable phase after calcination between 550 and 700 °C [16]. No other manganese phases were evident in this temperature range.

On the other hand, it should be noted that the X-ray diffraction patterns did not show the presence of any detectable crystal-like phase of manganese oxides, namely Mn_2O_3, on Mn(1.0%)/H-ZSM-5 and Mn(4.3%)/H-ZSM-5

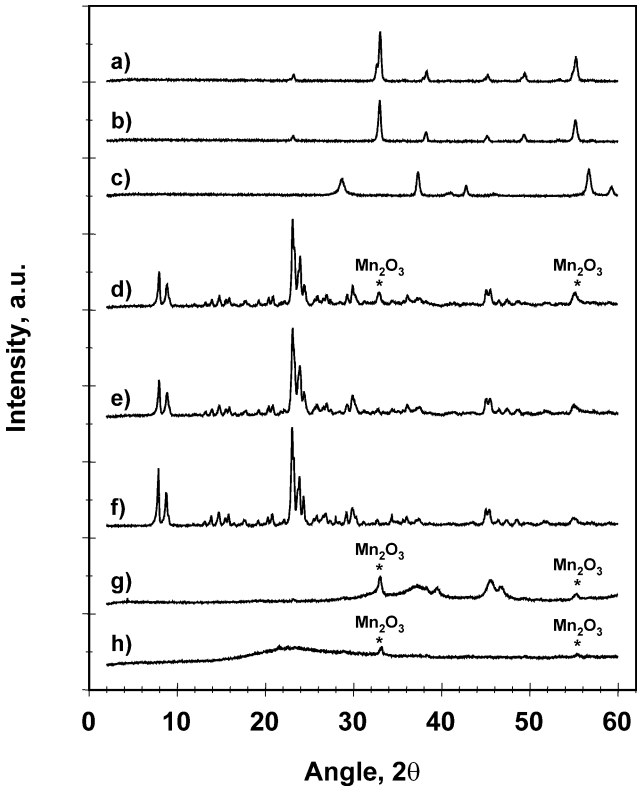

Fig. 1. XRD spectra: (a) MnO_2 ($Mn(NO_3)_2 \cdot 4H_2O$ calcined at 400 °C/3 h/air), (b) Mn_2O_3 ($Mn(NO_3)_2 \cdot 4H_2O$ calcined at 550 °C/3 h/air), (c) Mn_2O_3 ($Mn(NO_3)_2 \cdot 4H_2O$ calcined at 700 °C/3 h/air), (d) Mn(8.3%)/H-ZSM-5, (e) Mn(4.3%)/H-ZSM-5, (f) Mn(1.0%)/H-ZSM-5, (g) Mn(4.3%)/Al_2O_3, (h) Mn(4.2%)/SiO_2.

catalysts. The lack of X-ray diffraction lines of characteristic Mn_2O_3 indicated that the H-ZSM-5-supported manganese species were highly dispersed [17]. Nevertheless, the most intense peaks of Mn_2O_3 crystals were noticeable for Mn(8.3%)/H-ZSM-5, revealing that large crystallites were eventually formed. The XRD patterns of the Mn/H-ZSM-5 catalysts were essentially identical to those of the H-ZSM-5 support, except for a certain loss (10–15%) in the intensity of principal diffraction lines, which was more remarkable with increasing Mn content. This pointed out that the ZSM-5 structure was largely maintained after the addition of manganese to the support.

Table 1 lists the textural properties of the catalysts along with the manganese loading. For the sake of clarity the weight contents of the metal and metal oxide were included. It was noted that the incorporation of increasing amounts of manganese to H-ZSM-5 zeolite slightly diminished its surface area, as well as its pore volume. The surface area of H-ZSM-5 zeolite was 50 $m^2\,g^{-1}$ greater than that of Mn(8.3%)/H-ZSM-5 catalyst, suggesting that some pore blockage might have occurred due to high metal loading. This slight loss of surface area was evidence that the microporous character of H-ZSM-5 zeolite was hardly modified after impregnation, as also revealed by XRD data.

Temperature-programmed desorption of ammonia was used to determine the number and the strength of the acid sites present in the metal-modified catalysts (Table 1). The area under the TPD profile dropped significantly for all the metal loaded zeolite catalysts compared with the parent H-ZSM-5 zeolite, thereby showing an overall loss of the total number of acid sites with increasing manganese addition. Analyzing the NH_3-TPD profiles (Fig. 2), it could be observed that the first maximum at 150 °C, corresponding to weak acid sites, was roughly the same for all the zeolite catalysts. The second maximum at 350–375 °C, associated with medium-strength acidity, decreased noticeably. Moreover, a third maximum was observed at 500 °C in the case of manganese oxide-based zeolite catalysts, whereas this additional peak was not detectable with H-ZSM-5 [18]. The low concentration of this third very strong acid site compared with the remaining acid sites suggested that these species were created by the metal cations. The population of this type of acid sites increased with increasing manganese content [19]. As a conclusion, total acidity of Mn-impregnated H-ZSM-5 catalysts was found to be a combined effect of two factors: first, Brønsted acidity due to negatively charged AlO_4 tetrahedra and second, cationic acidity due to incorporated manganese.

TPR patterns of the metal-loaded zeolite catalysts as function of Mn loading are presented in Fig. 3. A two-step reduction profile was observed for all the zeolites, except for the pure protonic sample. The two reduction peaks were consistent with successive reduction of Mn_2O_3 into Mn_3O_4, followed by a final reduction to MnO [17]. TPR measurements were characteristic of bulk Mn_2O_3 species. It was observed

Table 1
Physicochemical properties of the supports and the manganese oxide-based catalysts

Catalyst [a]	Mn content	Mn_2O_3 content	Surface area	Pore volume	Total acidity	Acid sites (%)		
	(wt%)	(wt%)	($m^2\,g^{-1}$)	($cm^3\,g^{-1}$)	(mmol $NH_3\,g^{-1}$)	Weak	Medium	Strong
Mn(1.0%)/H-ZSM-5	1.0	0.01	423	0.232	0.43	57.7	32.4	9.8
Mn(4.3%)/H-ZSM-5	4.3	0.06	413	0.225	0.56	44.5	36.4	19.1
Mn(8.3%)/H-ZSM-5	8.3	0.12	410	0.232	0.50	43.0	37.6	19.5
Mn(4.3%)/Al_2O_3	4.3	0.06	103	0.564	0.34	88.4	11.6	–
Mn(4.2%)/SiO_2	4.2	0.06	300	1.095	–	–	–	–
H-ZSM-5	–	–	460	0.230	0.58	43.8	56.2	–
Al_2O_3	–	–	105	0.571	0.35	85.8	14.2	–
SiO_2	–	–	323	1.203	–	–	–	–

[a] All the samples were calcined at 550 °C in air for 3 h.

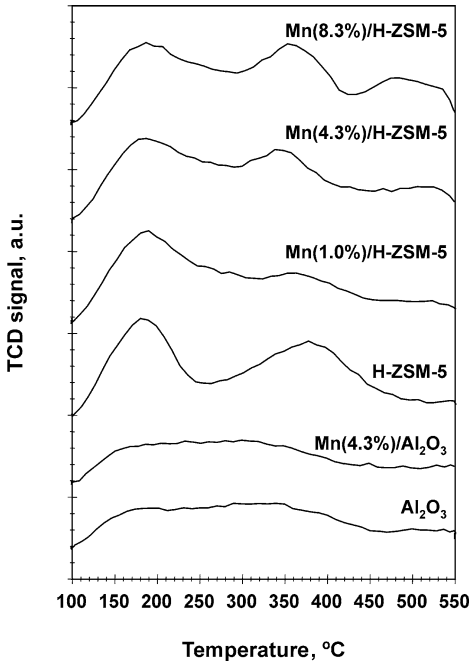

Fig. 2. Temperature-programmed desorption of ammonia profiles of various catalysts and supports.

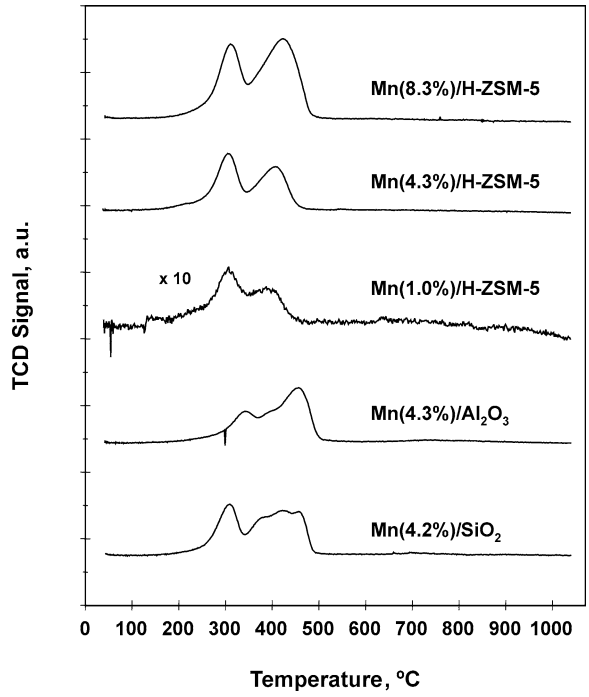

Fig. 3. Temperature-programmed reduction patterns of various supported manganese oxide catalysts.

that both reduction peaks slightly shifted to higher temperatures with increasing content. Hence, the reduction peaks appeared at 310 and 410 °C on Mn(4.3%)/H-ZSM-5, and 320 and 430 °C on Mn(8.3%)/H-ZSM-5. The Mn(1.0%)/H-ZSM-5 zeolite also exhibited minor features at 300 and 400 °C. Although XRD analysis did not reveal crystalline material, small Mn_2O_3 clusters are thought to be present in a highly dispersed form on the outer surface of Mn/H-ZSM-5 catalysts with a low metal content. As suggested by the increased reduction temperatures and the presence of diffraction peaks corresponding to metallic clusters, the higher Mn loading, the more aggregated Mn_2O_3 crystals were formed resulting in a poorer dispersion.

3.2. Activity tests

Before studying the catalytic behavior of H-ZSM-5-supported manganese oxide catalysts, first a comparative study was carried out in order to assess the better catalytic properties of H-ZSM-5 zeolite as support in comparison with those of other typical commercial supports such as alumina and silica. For this purpose, Mn(4.3%)/Al_2O_3 and Mn(4.2%)/SiO_2 catalysts were prepared by impregnation of γ-alumina SCM-129X (Rhône Poulenc) and silica CS-1030-E (PQ Corporation) supports, respectively, with an aqueous solution of manganese nitrate and subsequent drying at 120 °C for 5 h and calcination in air at 550 °C for 3 h. The physiochemical properties of these catalysts are listed in Table 1. As can be observed, Mn(4.3%)/H-ZSM-5, Mn(4.3%)/Al_2O_3, and Mn(4.2%)/SiO_2 catalysts had roughly the same cation content. The total acidity of alumina and silica supports was noticeably lower than that of H-ZSM-5 zeolite (Table 1). Moreover, the impregnation of manganese did not affect the acid strength distribution. Results from XRD and TPR of Mn(4.3%)/Al_2O_3 and Mn(4.2%)/SiO_2 catalysts revealed the presence of relatively large crystals of Mn_2O_3 species (Fig. 1), which required higher temperatures for complete reduction (Fig. 3). Consequently, the metallic dispersion of these catalysts appeared to be poorer compared with Mn(4.3%)/H-ZSM-5 catalyst.

Typically the catalytic activity was characterized by monitoring the combustion efficiency as a function of temperature for a particular VOC at given test conditions. A characteristic S-shaped curve, which is called light-off or ignition curve, was obtained. T_{50} (temperature at which 50% conversion is attained) was used as a criterion for comparing the catalytic activity for various catalysts. The light-off curves of the decomposition of DCM and TCE over these three Mn_2O_3-based catalysts are shown in Figs. 4 and 5, respectively. It was observed that all the catalyzed reactions required lower reaction temperatures than the homogeneous reaction irrespective of catalyst composition or type of feed. The Mn(4.3%)/H-ZSM-5 catalyst produced 50% conversion of DCM at 340 °C while Mn(4.3%)/Al_2O_3 and Mn(4.2%)/SiO_2 required a temperature increase to 400 and 440 °C, respectively, for a similar conversion level. On the other hand, the Mn(4.3%)/H-ZSM-5 catalyst achieved 50% TCE conversion at temperatures as low as 300 °C where the other two manganese-based catalysts needed a minimum temperature of 425 °C (Mn(4.3%)/Al_2O_3) and 445 °C (Mn(4.2%)/SiO_2) to produce 50% conversion. Thus, according to the T_{50} values for the oxidation of both chlorinated hydrocarbons, there was a decreasing activity of the

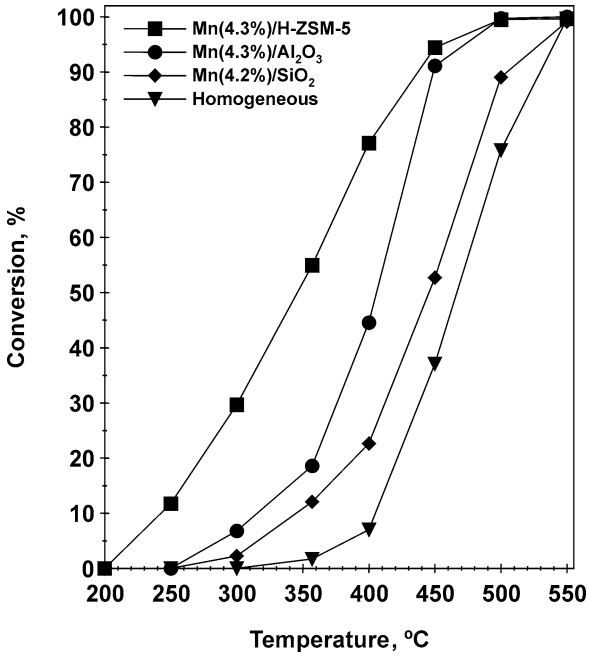

Fig. 4. DCM oxidation light-off curves over Mn(4.3%)/H-ZSM-5, Mn(4.3%)/Al_2O_3, Mn(4.2%)/SiO_2, and empty reactor (homogeneous reaction).

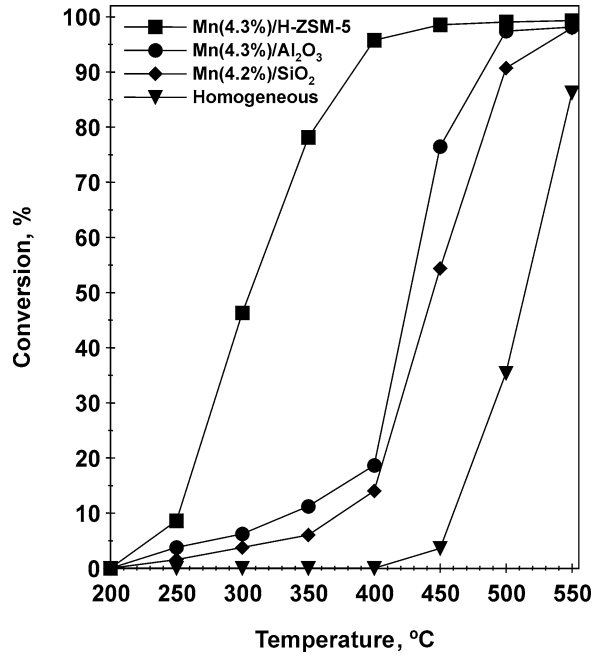

Fig. 5. TCE oxidation light-off curves over Mn(4.3%)/H-ZSM-5, Mn(4.3%)/Al_2O_3, Mn(4.2%)/SiO_2, and empty reactor (homogeneous reaction).

various catalysts in the following order: Mn(4.3%)/H-ZSM-5 > Mn(4.3%)/Al_2O_3 > Mn(4.2%)/SiO_2 > homogeneous reaction. This activity trend perfectly correlated with the order of the catalysts as a function of their total acidity pointing out that the activity of supported manganese oxide catalysts strongly depended on the nature of the support. Furthermore, polyvalent cations present in the zeolite framework also improved the zeolite acidity by creating highly strong acidic sites. On the other hand, the higher metallic dispersion of Mn(4.3%)/H-ZSM-5, as shown by TPR, also resulted in a better catalytic behavior. In contrast, the low activity of alumina and silica based catalysts was associated with the low acidity of these catalytic supports, which was hardly enhanced with Mn loading as revealed by NH_3-TPD, and with a poorer dispersion of Mn_2O_3 clusters. Oxygen uptake measurements were also consistent with the observed activity results since Mn(4.3)%/H-ZSM-5 exhibited the largest adsorption capacity with a value of 0.27 mmol O_2 g^{-1} in comparison with 0.12 and 0.10 mmol O_2 g^{-1} for Mn(4.3%)/Al_2O_3 and Mn(4.2%)/SiO_2, respectively.

Taking into account the conversion data from the decomposition runs without any catalyst and with manganese oxide supported on alumina and silica, TCE appeared to be a more stable compound with respect to DCM, requiring higher temperatures to complete combustion. Surprisingly, TCE conversion was noticeably accelerated when using Mn(4.3%)/H-ZSM-5 as catalyst since a T_{50} value as low as 300 °C was noted while T_{50} for DCM combustion was 340 °C. Perhaps possible structural and reaction mechanism differences between the chlorinated VOCs led to differences in reactivity of Mn(4.3%)/H-ZSM-5 catalyst.

In order to establish an optimal metal loading, Mn(1.0%)/H-ZSM-5 and Mn(8.3%)/H-ZSM-5 along with Mn(4.3%)/H-ZSM-5 zeolite catalysts were evaluated for the oxidation of DCM and TCE. As indicated in Figs. 6 and 7, the manganese incorporation to the zeolite induced an important reduction in T_{50} values for chlorocarbon oxidation with respect to pure H-ZSM-5, which varied depending on the metal content. It is worth noting that the H-ZSM-5 zeolite catalyst did have some activity, this being considerably higher than the homogeneous conversion results for both chlorinated compounds. In fact, under the existing conditions no detectable homogeneous reaction occurred at temperatures below 350–400 °C for DCM and 450–500 °C for TCE.

As for DCM, catalytic activity was found to decrease in the following order: Mn(4.3%)/H-ZSM-5 > Mn(1.0%)/H-ZSM-5 ≈ Mn(8.3%)/H-ZSM-5 > H-ZSM-5. The decrease in T_{50} with respect to the H-ZSM-5 zeolite ranged from 60 °C over Mn(4.3%)/H-ZSM-5 to 40 °C over Mn(1.0%)/H-ZSM-5 and Mn(8.3%)/H-ZSM-5. The differences in activity were discernible only at temperatures below 400 °C.

According to TCE destruction efficiency, the zeolite catalysts could be listed as Mn(4.3%)/H-ZSM-5 ≈ Mn(8.3%)/H-ZSM-5 ≫ Mn(1.0%)/H-ZSM-5 > H-ZSM-5. Interestingly, Mn(4.3%)/H-ZSM-5 and Mn(8.3%)/H-ZSM-5 zeolite catalysts showed a remarkable improvement in conversion, which increased from as low as 15% over Mn(1%)/H-ZSM-5 and H-ZSM-5 to almost 95% over Mn(5%)/H-ZSM-5 and Mn(10%)/H-ZSM-5 at 400 °C. This conversion

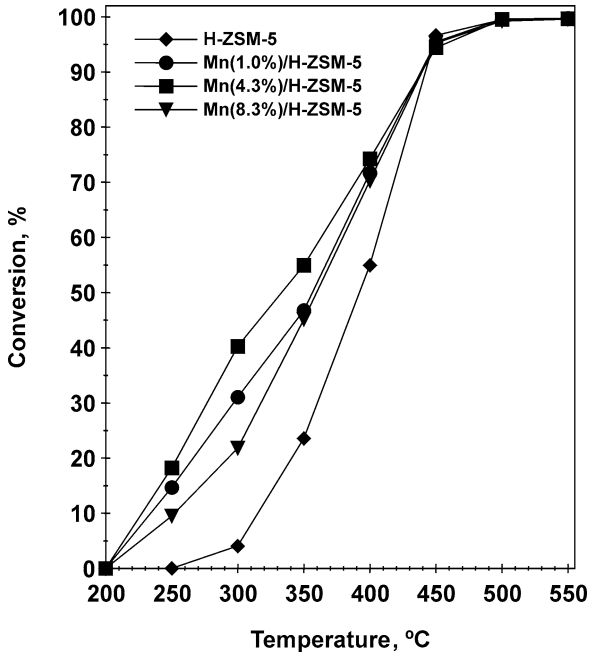

Fig. 6. DCM oxidation light-off curves over Mn/H-ZSM-5 catalysts for various loadings.

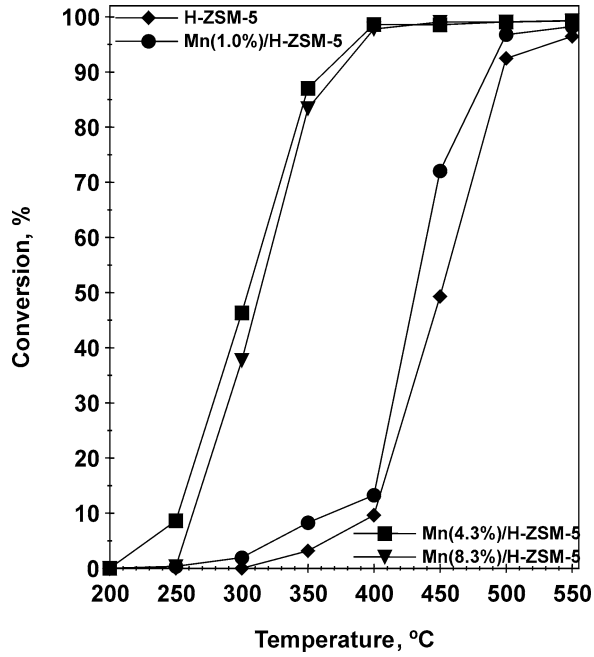

Fig. 7. TCE oxidation light-off curves over Mn/H-ZSM-5 catalysts for various loadings.

difference signified the importance of the presence of relatively high loadings of Mn_2O_3 as catalyst agent for TCE destruction. It was also seen that the catalytic activity slightly decreased for a further increase of Mn loading from 4.3 to 8.3 wt%.

Taken together, the chlorinated VOC conversion results demonstrate that 4.3 wt% was an optimal amount of manganese on H-ZSM-5 for the oxidative decomposition of both dichloromethane and trichloroethylene. The catalytic activity did not increase linearly with manganese loading when Mn content was higher than 4.3 wt%, owing to the fact that the amount necessary for monolayer coverage was probably exceeded and therefore the surface of highly dispersed Mn_2O_3 was no longer increased [10]. As revealed by TPR results, the dispersion of Mn(4.3%)/H-ZSM-5 appeared to be higher than that of Mn(8.3%)/H-ZSM-5. The oxygen chemisorption capacity of this catalyst was higher than that of Mn(8.3%)/H-ZSM-5 catalyst (0.23 mmol O_2 g^{-1}). It is worth noting that surface area of the zeolite catalysts did not seem to control the activities of the catalysts, as differences in the surface area values, as listed in Table 1, were observed with no corresponding trend in activity.

3.3. Product distribution

Apart from analyzing the catalytic activity for chlorinated VOC destruction, the product distribution of H-ZSM-5-supported manganese oxide catalysts was also monitored. The main oxidation products formed were CO, CO_2, HCl, and Cl_2 [14,20]. Additionally, when oxidizing DCM small amounts of methyl chloride were detected at mild temperatures (300–400 °C) [21]. The peak concentration of this by-product was 95 and 165 ppm over Mn(1.0%)/H-ZSM-5 and H-ZSM-5 catalysts, respectively. At higher temperatures the concentration decreased, and thus this compound was completely decomposed at 500 °C. In contrast, methyl chloride was no longer detected in the temperature range studied over zeolite catalysts with higher Mn content. As regards TCE oxidation, small amounts of tetrachloroethylene were detected as a by-product in the product stream [22]. The peak concentrations were 60, 200, 280, and 390 ppm over H-ZSM-5, Mn(1.0%)/H-ZSM-5, Mn(4.3%)/H-ZSM-5, and Mn(8.3%)/H-ZSM-5, respectively. Since tetrachloroethylene was presumably generated by chlorination, its formation was favored when reactive Cl_2 was present in large quantities [23], as will be noted later. This occurred for TCE oxidation catalyzed by Mn(4.3%)/H-ZSM-5 and Mn(8.3%)/H-ZSM-5 catalysts.

DCM contains sufficient hydrogen associated with the parent molecule to yield hydrogen chloride exclusively. Unexpectedly, significant amounts of molecular chlorine were observed above 400 °C. The Cl_2 was believed to arise from the oxidation of hydrogen chloride at high temperatures, the Deacon reaction ($2HCl + \frac{1}{2}O_2 \rightleftharpoons Cl_2 + H_2O$). Cl_2 production via the Deacon reaction was promoted with increasing manganese content, thus revealing its high activity for this reaction. Hence, the maximum concentration at 550 °C was 320, 360, 580, and 605 ppm over H-ZSM-5, Mn(1.0%)/H-ZSM-5, Mn(4.3%)/H-ZSM-5, and Mn(8.3%)/H-ZSM-5, respectively. Unlike DCM, in the case of TCE there is no sufficient hydrogen associated with the parent molecule to yield HCl exclusively. As a result, a noticeable chlorine formation was noted, this being more remarkable over Mn(4.3%)/H-

ZSM-5 and Mn(8.3%)/H-ZSM-5 catalysts resulting in chlorine concentrations higher than 800 ppm.

As far as CO and CO_2 formation in chlorinated VOC conversion was concerned, a common feature of the formation of CO_2 over CO was observed at high conversion levels. The low selectivity toward CO_2 ($< 50\%$ at 550 °C) for pure H-ZSM-5 zeolite suggested that the zeolites did not promote the deep oxidation to CO_2 [22]. However, increasing the manganese oxide loading on the H-ZSM-5 support remarkably increased the CO_2 selectivity due to the high activity of Mn for CO oxidation reaction ($CO + \frac{1}{2}O_2 \rightarrow CO_2$) [24]. Hence, selectivity values to CO_2 higher than 95% were obtained over Mn(4.3%)/H-ZSM-5 and Mn(8.3%)/H-ZSM-5 catalysts. Carbon balances were typically greater than 95% for all runs reported in this study.

In conclusion, among H-ZSM-5 zeolite, alumina, and silica supports, Mn_2O_3 supported on H-ZSM-5 was found to exhibit the highest activity for chlorinated VOC combustion. The better catalytic behavior of Mn/H-ZSM-5 catalyst was attributed to a higher acidity of H-ZSM-5 support, which was enhanced by Mn incorporation, to a higher dispersion of the metallic species, and to a higher oxygen chemisorption capacity. An optimal manganese loading of 4.3 wt% was observed to efficiently oxidize both single and double carbon chlorinated feeds at temperatures between 400 and 450 °C. The main oxidation products were carbon monoxide, carbon dioxide, hydrogen chloride, and chlorine. CO_2 and Cl_2 selectivities were promoted with increasing manganese content. This was interpreted in terms of the high activity of Mn in both CO oxidation and Deacon reaction.

Acknowledgments

The authors thank Universidad del Pais Vasco/EHU (9/UPV 13517/2001) and Ministerio de Ciencia y Tecnología for the financial support (PPQ2001-0543).

References

[1] H. Sidebottom, J. Franklin, Pure Appl. Chem. 68 (1996) 1757.
[2] E.C. Moretti, Practical Solutions for Reducing Volatile Organic Compounds and Hazardous Air Pollutants, CWRT AIChE, New York, 2001.
[3] S. Krishnamoorthy, J.A. Rivas, M.D. Amiridis, J. Catal. 193 (2002) 364.
[4] S.K. Agarwal, J.J. Spivey, J.B. Butt, Appl. Catal. 81 (1992) 239.
[5] S. Chatterjee, H.L. Greene, Y.J. Park, J. Catal. 138 (1992) 179.
[6] R. Rachapudi, P.S. Chintawar, H.L. Greene, J. Catal. 185 (1999) 58.
[7] J.J. Spivey, J.B. Butt, Catal. Today 11 (1992) 456.
[8] D.-C. Kim, S.-K. Ihm, Environ. Sci. Technol. 35 (2001) 222.
[9] E. Finocchio, G. Busca, Catal. Today 70 (2001) 213.
[10] Y. Liu, M. Luo, Z. Wei, Q. Xin, P. Ying, C. Li, Appl. Catal. B 29 (2001) 61.
[11] E. Kantzer, D. Döbber, D. Kiebling, G. Wendt, Stud. Surf. Sci. Catal. 143 (2002) 489.
[12] H. Greene, D. Prakash, K. Athota, G. Atwood, C. Vogel, Catal. Today 27 (1996) 289.
[13] R. López-Fonseca, S. Cibrián, J.I. Gutiérrez-Ortiz, J.R. González-Velasco, Stud. Surf. Sci. Catal. 142 (2002) 841.
[14] R. López-Fonseca, A. Aranzabal, J.I. Gutiérrez-Ortiz, J.I. Álvarez-Uriarte, J.R. González-Velasco, Appl. Catal. B 30 (2001) 303.
[15] J.R. González-Velasco, A. Aranzabal, J.I. Gutiérrez-Ortiz, R. López-Fonseca, M.A. Gutiérrez-Ortiz, Appl. Catal. B 19 (1998) 189.
[16] M. Baldi, V. Sánchez-Escribano, J.M. Gallardo-Amores, F. Milella, G. Busca, Catal. Today 17 (1998) L175.
[17] F. Kapteijn, A.D. van Langeveld, J.A. Moulijn, A. Andreini, M.A. Vuurman, A.M. Turek, I.E. Jehng, J.-M. Wachs, J. Catal. 150 (1994) 94.
[18] B. Wichterlova, S. Beran, S. Bednarova, K. Nedomova, L. Dudikova, P. Jiru, Stud. Surf. Sci. Catal. 37 (1988) 199.
[19] D.J. Parrillo, C. Pereira, G.T. Kokotailo, R.J. Gorte, J. Catal. 138 (1992) 377.
[20] R. López-Fonseca, A. Aranzabal, P. Steltenpohl, J.I. Gutiérrez-Ortiz, J.R. González-Velasco, Catal. Today 62 (2000) 367.
[21] R. López-Fonseca, J.I. Gutiérrez-Ortiz, M.A. Gutiérrez-Ortiz, J.R. González-Velasco, J. Catal. 209 (2002) 145.
[22] R. López-Fonseca, J.I. Gutiérrez-Ortiz, M.A. Gutiérrez-Ortiz, J.R. González-Velasco, J. Appl. Chem. Biotechnol. 78 (2003) 15.
[23] J.R. González-Velasco, A. Aranzabal, R. López-Fonseca, R. Ferret, J.A. González-Marcos, Appl. Catal. B 24 (2000) 33.
[24] J. Carnö, M. Ferrandon, E. Björnbom, S. Järäs, Appl. Catal. A 155 (1997) 265.